MOLECULAR AND CELLULAR BIOLOGY, June 2002, p. 4358–4365 Vol. 22, No. 12
0270-7306/02/$04.00+0 DOI: 10.1128/MCB.22.12.4358–4365.2002

PEX11β Deficiency Is Lethal and Impairs Neuronal Migration but Does Not Abrogate Peroxisome Function

Xiaoling Li,[1] Eveline Baumgart,[1] James C. Morrell,[1] Gerardo Jimenez-Sanchez,[2] David Valle,[2] and Stephen J. Gould[1]*

Department of Biological Chemistry[1] and The Howard Hughes Medical Institute and Departments of Pediatrics and Molecular Biology and Genetics,[2] The Johns Hopkins University School of Medicine, Baltimore, Maryland 21205

Received 23 January 2002/Returned for modification 25 February 2002/Accepted 5 March 2002

Zellweger syndrome is a lethal neurological disorder characterized by severe defects in peroxisomal protein import. The resulting defects in peroxisome metabolism and the accumulation of peroxisomal substrates are thought to cause the other Zellweger syndrome phenotypes, including neuronal migration defects, hypotonia, a developmental delay, and neonatal lethality. These phenotypes are also manifested in mouse models of Zellweger syndrome generated by disruption of the *PEX5* or *PEX2* gene. Here we show that mice lacking peroxisomal membrane protein PEX11β display several pathologic features shared by these mouse models of Zellweger syndrome, including neuronal migration defects, enhanced neuronal apoptosis, a developmental delay, hypotonia, and neonatal lethality. However, *PEX11*β deficiency differs significantly from Zellweger syndrome and Zellweger syndrome mice in that it is not characterized by a detectable defect in peroxisomal protein import and displays only mild defects in peroxisomal fatty acid β-oxidation and peroxisomal ether lipid biosynthesis. These results demonstrate that the neurological pathologic features of Zellweger syndrome can occur without peroxisomal enzyme mislocalization and challenge current models of Zellweger syndrome pathogenesis.

Peroxisomes are single-membrane bound metabolic organelles that are present in all eukaryotic cells. In their lumen reside the enzyme systems responsible for a wide variety of metabolic pathways, including the β-oxidation of very long-chain fatty acids (VLCFAs), α- and β-oxidation of branched-chain fatty acids, biosynthesis of ether linked lipids and cholesterol, synthesis of bile acids, metabolism of polyunsaturated fatty acids, and H_2O_2 metabolism (25, 36). The importance of peroxisomes for human health is best demonstrated by the existence of Zellweger syndrome, a lethal neurological disorder characterized by defects in peroxisomal matrix enzyme import (30). This defect negatively impacts virtually all peroxisomal metabolic functions, which leads, in turn, to the accumulation of peroxisomal α- and β-oxidation substrates (e.g., phytanic acid and VLCFAs, respectively) and reduced levels of ether-linked lipids (e.g., plasmalogens) (11). Zellweger syndrome is also associated with severe defects in mitochondrial structure and function (5, 10), as well as a pleiotropic set of clinical phenotypes, including a developmental delay, hypotonia, neuronal migration defects, enhanced neuronal apoptosis, and an array of hepatic and renal abnormalities (11).

There is uncertainty regarding the etiologic agent(s) and mechanisms responsible for the neuronal migration defect and other phenotypes of Zellweger syndrome. However, the accumulation of toxic peroxisomal α- and β-oxidation substrates or depletion of peroxisomal products, such as ether-linked lipids, have been proposed to cause its pathologic features (28). In contrast to the uncertainty regarding Zellweger syndrome pathogenesis, the molecular genetics of Zellweger syndrome and its milder variants (neonatal adrenoleukodystrophy and infantile Refsum disease) are well understood (11, 30). These peroxisome biogenesis disorders are inherited in an autosomal recessive fashion and are caused by mutations in any of at least 12 distinct *PEX* genes (11). Approximately 20 *PEX* genes are required for peroxisome biogenesis, and with the exception of *PEX11*, all are required for peroxisomal matrix enzyme import (30). PEX11 proteins are components of the peroxisomal membrane in a wide array of species, including yeast, protozoan parasites, and mammals (1, 2, 6, 19, 21, 27, 32, 34). They appear to play an important role in peroxisome division, although the nature of their role is currently the subject of debate. In one model, PEX11 proteins are thought to play a direct role in peroxisome division (6, 12, 21, 27, 34). Recently, another model was proposed in which PEX11 proteins play a direct role in medium-chain fatty acid oxidation and only affect peroxisome division indirectly through this metabolic role (35).

Mammals express at least two *PEX11* genes, the inducible *PEX11*α gene and the constitutively expressed *PEX11*β gene (1, 2, 27, 34). Here we report an analysis of mice that lack the *PEX11*β gene. Quite unexpectedly, we found that *PEX11*$\beta^{-/-}$ mice exhibit numerous Zellweger syndrome pathologic features, including a developmental delay, hypotonia, neuronal migration defects, and enhanced neuronal apoptosis, even though they have no apparent defect in peroxisomal protein import and have only mild defects in peroxisomal metabolic function.

* Corresponding author. Mailing address: Department of Biological Chemistry, The Johns Hopkins University School of Medicine, 725 North Wolfe St., Baltimore, MD 21205. Phone: (410) 955-3424. Fax: (410) 955-0215. E-mail: sgould@jhmi.edu.

MATERIALS AND METHODS

Cloning and disruption of the murine *PEX11*β gene. A bacterial artificial chromosome (BAC) clone (no. 17747; Incyte Genomics Inc., St. Louis, Mo.) with the complete *PEX11*β gene was obtained by screening a BAC library of 129/svJ

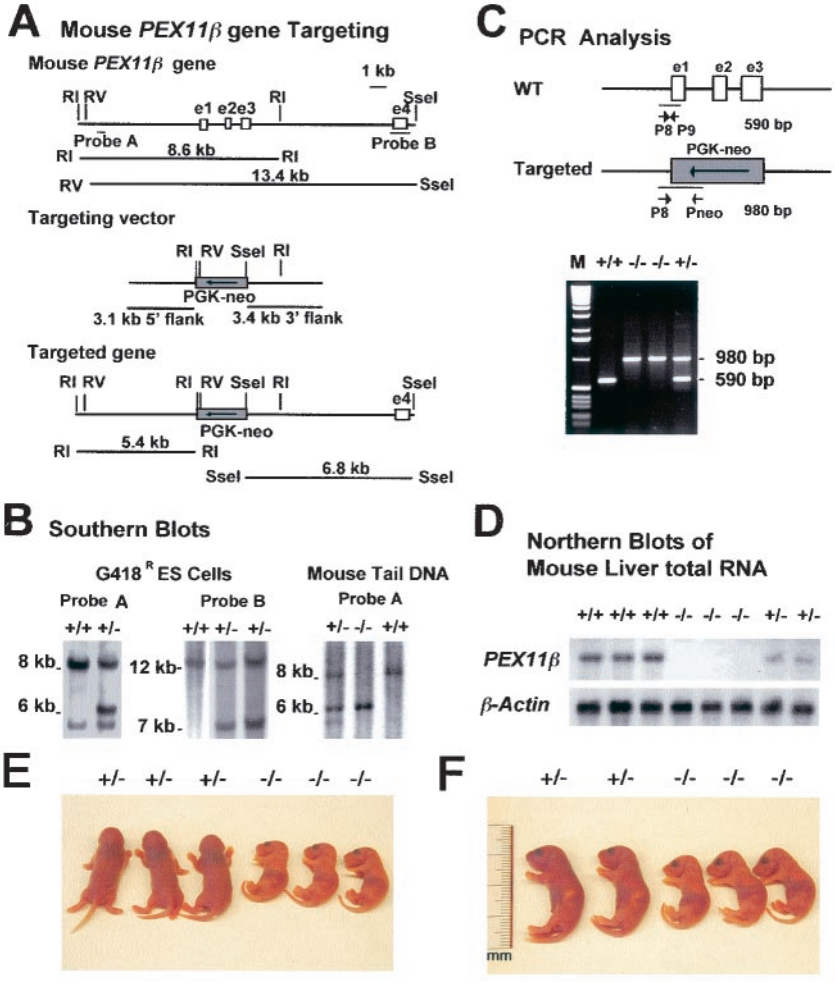

FIG. 1. Targeting of *PEX11*β. (A) Schematic representation of the *PEX11*β wild-type locus (top), the targeting vector (middle), and the targeted allele (bottom). Two flanking Southern blot probes, A and B, are indicated. (B) Southern blot analyses of the G418^r ES clone DNA with probes A and B and the mouse tail DNA with probe A. Probe A detects an 8.6-kb *Eco*RI fragment in the wild-type allele and a 5.4-kb fragment in the targeted allele. Probe B detects a 13.4-kb *Eco*RV/*Sse*I fragment in the wild-type allele and a 6.8-kb fragment in the targeted allele. (C) PCR analysis of mouse tail DNA. Positions of the primers are indicated. The wild-type (WT) allele product is 590 bp, and the targeted-allele product is 980 bp. M, molecular size markers. (D) Northern blot analysis of total liver RNA from wild-type (+/+), homozygous (−/−), and heterozygous (+/−) animals. The Northern blot shown was probed with a radioactively labeled murine *PEX11*β cDNA probe (top), stripped, and probed with labeled β-actin cDNA (bottom). (E and F) *PEX11*β$^{-/-}$ mice display intrauterine growth retardation and are hypotonic. One litter of newborn mice with heterozygous (+/−) and homozygous (−/−) offspring is depicted either in the conscious state (E) or under ether anesthesia (F).

mouse genomic DNA with the full-length murine *PEX11*β cDNA (34). *Eco*RI-*Xba*I, *Xba*I, or *Hin*dIII-fragments spanning a 13-kb region containing the *PEX11*β gene were subcloned into pLITMUS vectors (New England BioLabs, Beverly, Mass.) and sequenced. The targeting vector, designed to disrupt the first three exons of the *PEX11*β gene (Fig. 1A), was generated by insertion of *Apa*LI-*Sma*I (3.1-kb *PEX11*β 5′ untranslated region) and *Hin*dIII-*Not*I (3.4 kb of intron 3) fragments into pGT-N29 as the 5′- and 3′-flanking regions of the pgk-Neo cassette. A 200-μg sample of targeting vector-DNA was linearized with *Swa*I and electroporated into 6.5×10^6 R1 embryonic stem (ES) cells as previously described (40). After selection with G418 at 200 μg/ml, recombined ES cell clones were identified by mini-Southern blot hybridization analysis of *Eco*RI- or *Eco*RV-*Sse*I-digested ES cell genomic DNA with two flanking probes. Four *PEX11*β$^{+/-}$ ES cell clones were injected into blastocysts of C57BL/6 host mice. Chimeric males from three different ES cell lines were intercrossed with C57BL/6 mice (Jackson Laboratory, Bar Harbor, Maine), and agouti offspring were tested for the presence of the gene disruption by Southern blotting (33). Heterozygous F_1 mice were backcrossed with C57BL/6 mice for five generations. Genotypes of mice from generation F_2 and beyond were determined by PCR with primer 8 (5′-GTCTAGGACAGGCTTCTGCTGTTC-3′), primer 9 (5′-GTTCCCCATCTTTCCCTTGAG-3′), and primer Neo (5′-ATATTGCTGAAGAGCTTGGCGGC-3′). Amplification reactions were done with 0.1 μg of DNA for the wild-type allele (primers 8 and 9 → 590 bp) or the targeted allele (primers 8 and Neo → 980 bp). For RNA blots, total RNA was isolated from mouse livers with the Purescript RNA isolation kit (Gentra Systems, Minneapolis, Minn.). RNA (10 μg/lane) was separated by electrophoresis on 1.5% formaldehyde-agarose gels, transferred to GeneScreen Plus membranes (NEN Life Science Products, Boston, Mass.), and hybridized in accordance with standard procedures (33).

MEF preparation and immunofluorescence assay. Mouse embryo fibroblasts (MEF) were isolated from E14.5 embryos as previously described (13). For indirect immunofluorescence assay, cells were fixed for 20 min in 3% formaldehyde in Dulbecco's phosphate-buffered saline (Life Technologies), pH 7.1; permeabilized for 5 min in 1% Triton X-100–Dulbecco's phosphate-buffered saline; and further processed as previously described (31). Affinity-purified rabbit anti-human PEX14 antibody has been described previously (31), sheep anti-human catalase antibodies were obtained from The Binding Site (Birmingham, United Kingdom), mouse monoclonal anti-myc antibodies were obtained from the supernatant of hybridoma 1-9E10 (7), and labeled secondary antibodies were obtained from standard commercial sources.

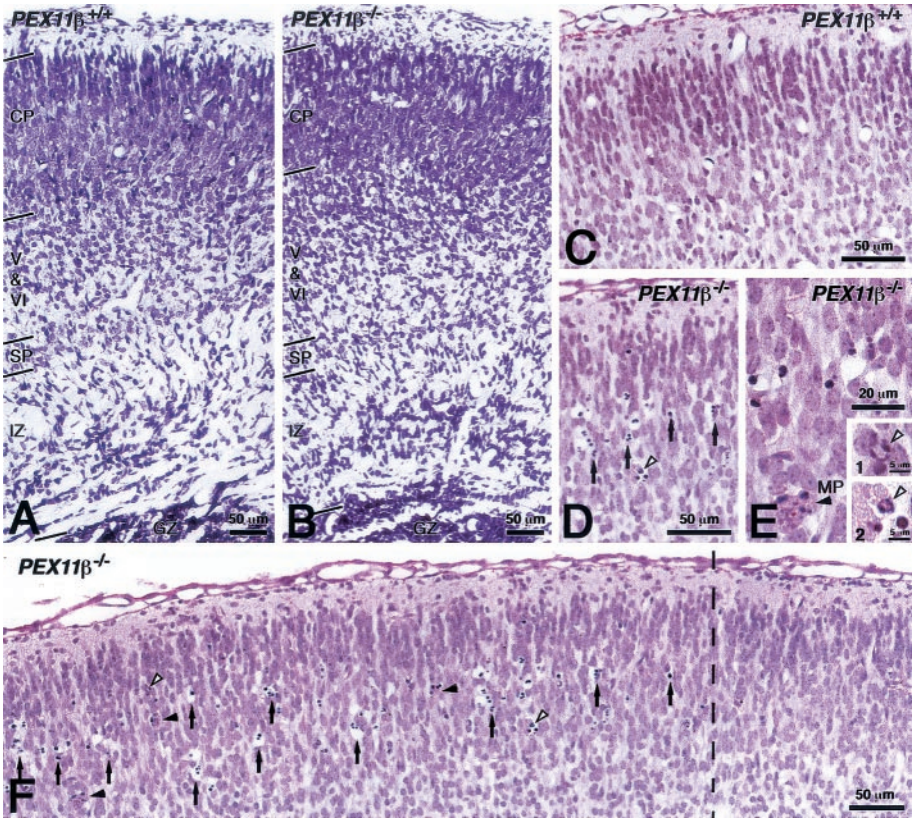

FIG. 2. Neuronal defects in *PEX11*β$^{-/-}$ mice. Carefully matched coronal (A and B; stained with cresyl fast violet) or sagittal (C to F; stained with PAS and hematoxylin) sections of control (A and C) and *PEX11*β$^{-/-}$ (B and D to F) mice in medial regions of the neocortex. In panel B, the neuronal migration defect is revealed by higher cell density in the intermediate zone (IZ) and layer V, as well as the altered structure and slightly lesser thickness of the cortical plate (CP). GZ, germinative zone; SP, subplate. Neuronal apoptoses of different stages are indicated by arrows (D to F). Insets 1 and 2 in panel E depict higher magnifications of early stages of chromatin condensation with typical nuclear cap structures of apoptotic cells, indicated by white arrowheads. Black arrowheads indicate macrophages (MP) (slightly more PAS positive) with phagocytosed material. Empty spaces are clearly visible where apoptotic neurons were located (D to F). In contrast, empty spaces in panel C represent endothelium-lined capillaries.

Histology and electron microscopy. Under ether anesthesia, mouse embryos (embryonic day 17.5 [E17.5] and E18.5) and newborn mice (postnatal day 0.5 [P0.5]) were perfusion fixed via the heart with 4% paraformaldehyde in phosphate-buffered saline, pH 7.4. Whole-mouse sections were obtained following overnight immersion fixation (OIF) at 4°C and paraffin embedding. Five-micrometer sagittal sections of whole mice were stained with hematoxylin and periodic acid-Schiff (PAS) for pathological analysis (3). For brain analysis, OIF was performed with opened skulls and the brains were removed and embedded in paraffin. Serial coronal sections (5 μm) were cut and stained with cresyl fast violet for pathological analysis (3). More than 200 carefully matched sections were examined for neuronal migration defects and apoptosis. For electron microscopy, cardiac perfusion fixation of newborn mice was performed with 4% paraformaldehyde–0.05% glutaraldehyde–2% sucrose–0.05% $CaCl_2$–0.1 M piperazine-*N*,*N*′-bis(2-ethanesulfonic acid) (PIPES) buffer, pH 7.4, followed by OIF in the same fixative without glutaraldehyde. Livers were removed, cut into 100-μm sections, and postfixed for 15 min with 1.0% glutaraldehyde in 0.1 M PIPES buffer. Catalase cytochemistry (30 min of preincubation and 2 h of incubation at 45°C) was performed with alkaline DAB medium as described by Fahimi (8). DAB-stained sections were postfixed with either aqueous or reduced osmium, embedded in Epon 812, and examined by electron microscopy.

Biochemical assays. Livers and brains (telencephalon) of newborn mice (P0.5) were weighed and homogenized in a tissue grinder with chloroform-methanol (2:1). Total lipids were extracted with 2:1:0.8 chloroform-methanol-water, converted to their methyl esters, dissolved in hexane at a concentration of ~1 μg/μl, and then separated by gas chromatography (DB-1 and SP-2560 columns) as previously described (24). The levels of VLCFAs and plasmalogens were calculated as percentages of the total fatty acids. Plasmalogen synthesis activity was determined in cultured MEF with the double-substrate, double-isotope method (with [^{14}C]hexadecanol and [^{3}H]hexadecyl-glycerol as substrates) (29). Fatty acid β-oxidation assays were carried out with [1-^{14}C]palmitic acid ($C_{16:0}$) and [1-^{14}C]lignoceric acid ($C_{24:0}$) as substrates in intact MEF (41). Branched-chain fatty acid (phytanic and pristanic acids) oxidation assays (41, 42) were done with cultured MEF with [2,3-^{3}H]phytanic acid or [1-^{14}C]pristanic acid as the substrate.

RESULTS

***PEX11*β$^{-/-}$ mice display neonatal lethality, intrauterine growth retardation, and hypotonia.** Exons 1 to 3 of the mouse *PEX11*β gene were disrupted in R1 ES cells by gene conversion with a *PEX11*β/pgk-Neo^{r} cassette (Fig. 1A). Correctly targeted *PEX11*β$^{+/-}$ cell lines were identified and injected into C57BL/6 blastocysts, and chimeric animals were generated. Chimeras were mated with C57BL/6 mice, and *PEX11*β$^{+/-}$ heterozygote animals were obtained from several chimeras and two independently generated *PEX11*β$^{+/-}$ ES cell lines (Fig. 1B and C). These mice were backcrossed to C57BL/6 mice five times to place the *PEX11*β disruption allele over a relatively homogeneous background. *PEX11*β$^{+/+}$, *PEX11*β$^{+/-}$, and *PEX11*β$^{-/-}$ fetuses were obtained in the expected Mendelian

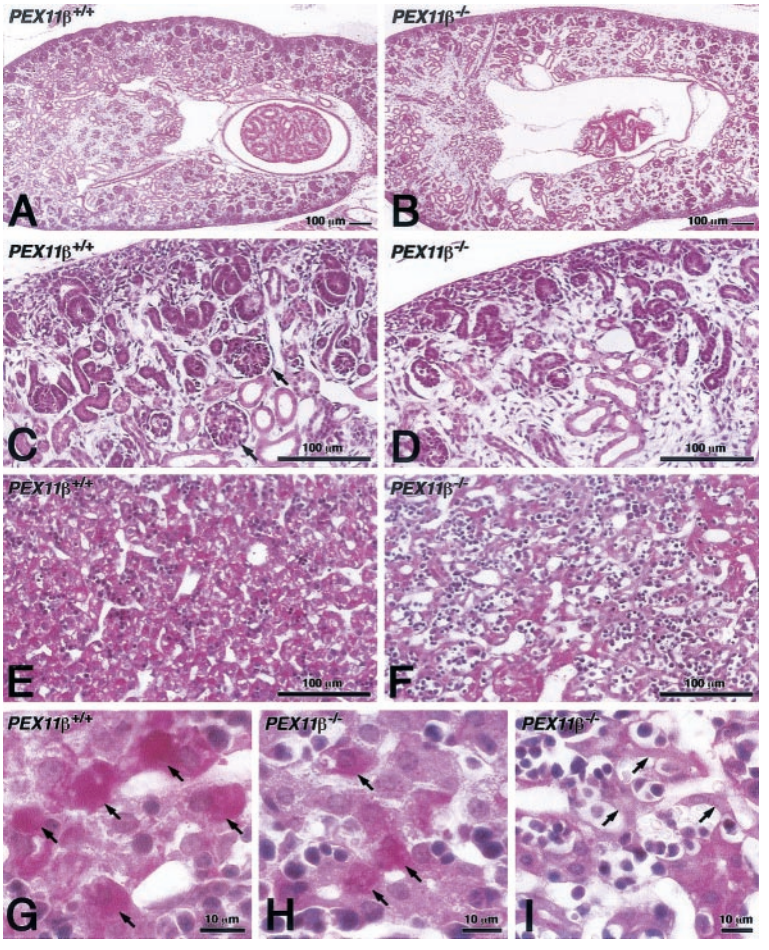

FIG. 3. Developmental delay in kidneys and livers of *PEX11*β$^{-/-}$ mice. Histological analysis of PAS- and hematoxylin-stained kidney (A to D) and liver (E to I) sections (5 μm) of P0.5 control (A, C, E, and G) and *PEX11*β$^{-/-}$ (B, D, F, H, and I) mice, depicting the strong delay in the development of both organs in *PEX11*β$^{-/-}$ animals. Well-developed glomeruli are present in control animals (C, arrows) but absent from *PEX11*β$^{-/-}$ animals (D). Tubules are also reduced in panel D. Livers of *PEX11*β$^{-/-}$ mice show regions of underdeveloped hepatocytes (F) with reduced glycogen (reduced PAS staining). Even areas with well-developed *PEX11*β$^{-/-}$ hepatocytes contained less glycogen (H) than did those of control animals (G). Arrows in panel H depict underdeveloped hepatocytes in *PEX11*β$^{-/-}$ mouse liver, which were not observed in controls.

ratios in intercrosses between *PEX11*β$^{+/-}$ animals. *PEX11*β$^{-/-}$ animals lack detectable *PEX11*β mRNA (Fig. 1D). Animals lacking *PEX11*β died shortly after birth on day 1, were undersized (~80% of wild-type size at P0.5) (Fig. 1E and F), were underweight (~60% of wild-type body weight at P0.5), were hypotonic (Fig. 1E), and suckled only poorly, as was evident from the reduced amounts of milk in their gastrointestinal tracts (Fig. 1F). No heterozygote phenotype was observed.

PEX11β$^{-/-}$ mice exhibit neuronal migration defects and a developmental delay. Neonatal hypotonia and neonatal lethality caused by defects in a peroxisomal membrane protein are unique characteristics of Zellweger syndrome. In addition, prior mouse models of Zellweger syndrome, which reproduce virtually all of the hallmarks of the human disease, also display the intrauterine growth defects we observed in *PEX11*β$^{-/-}$ mice (3, 9). Therefore, we investigated the possibility that *PEX11*β-deficient mice may display other pathologic characteristics of Zellweger syndrome. Zellweger syndrome is characterized by defective neuronal migration, and Zellweger syndrome mice display both a neuronal migration defect and enhanced apoptosis within the neocortex (11).

The neuronal migration defect of *PEX5*$^{-/-}$ mice is focal in nature and can be observed only in coronal sections through the neocortex (3) (E. Baumgart, unpublished data). In *PEX11*β$^{-/-}$ mice, we also detected focal areas of decreased neuronal migration in coronal sections of the neocortex. This neuronal migration defect is evident from the increased numbers of neurons in the intermediate zone and layer V, as well as structural alterations and slightly reduced thickness of the cortical plate (Fig. 2A and B). This was observed in all three *PEX11*β$^{-/-}$ mice that were examined and was not observed any of the three *PEX11*β$^{+/+}$ littermate control mice. Thus, the neuronal migration defect appeared to be a fully penetrant phenotype of *PEX11*β$^{-/-}$ mice. In addition, because *PEX11*β$^{-/-}$ mice display growth retardation and a developmental delay, we examined the neuronal migration defect in four *PEX11*β$^{-/-}$ embryos and four size-matched *PEX11*β$^{+/+}$ embryos. The neuronal migration defect was apparent in all four *PEX11*β$^{-/-}$ embryos and was not detected in any of the size-matched control embryos (data not shown).

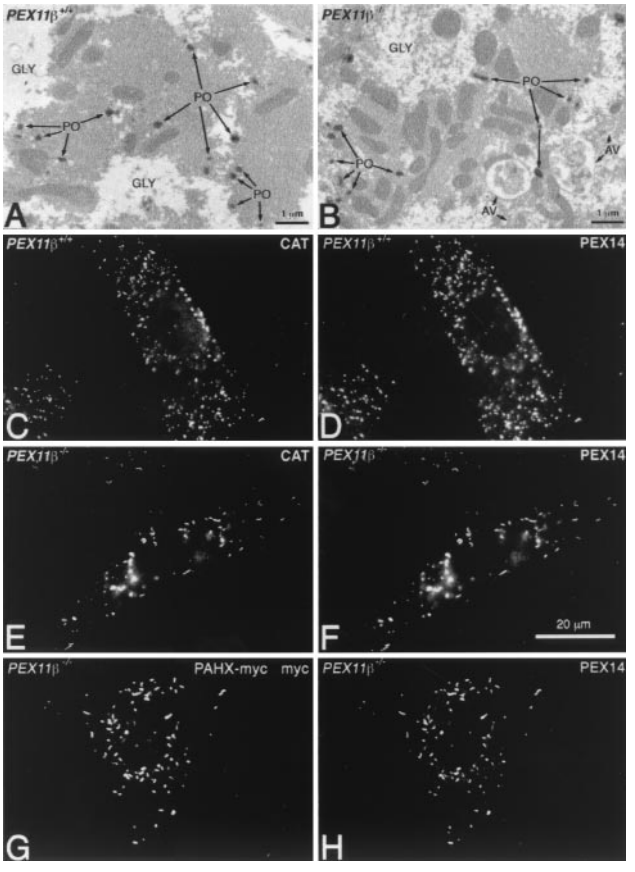

FIG. 4. PEX11β deficiency does not affect peroxisomal protein import. Ultrastructural analysis of hepatocytes from P0.5 control (A) and *PEX11*β$^{-/-}$ mice (B) shows normal import of the peroxisomal enzyme catalase, as determined by DAB staining (post-fixation with aqueous osmium). GLY, glycogen. (C to F) Indirect immunofluorescence analysis of control (C and D) and *PEX11*β$^{-/-}$ (E and F) MEF with antibodies to catalase (C and E) and PEX14 (D and F), a peroxisomal membrane protein. (G to H) Phytanoyl coenzyme A hydroxylase (PAHX)-myc targets to peroxisomes in *PEX11*β$^{-/-}$ fibroblasts. Cells were transfected with pcDNA3-PAHXmyc (22), grown for 2 days, and then processed for indirect immunofluorescence assay with a mouse monoclonal antibody to the myc epitope and rabbit anti-PEX14 antibodies.

Enhanced neuronal apoptosis was also observed in *PEX11*β$^{-/-}$ mice (Fig. 2C to F). Zellweger syndrome mice also exhibit a delay in renal development, and this too was observed in *PEX11*β$^{-/-}$ mice (Fig. 3A to D). Furthermore, we detected a focal mosaic pattern of a developmental delay and decreased glycogen in *PEX11*β$^{-/-}$ livers (Fig. 3E to I), although this could be due to the inability of *PEX11*β$^{-/-}$ mice to suckle properly. One other important feature of Zellweger syndrome is facial dysmorphism (25), but this was not observed in Zellweger syndrome mice. However, these mice did exhibit a developmental delay in calvarium ossification (9). *PEX11*β$^{-/-}$ animals also lack facial dysmorphism and exhibit a delay in the ossification of calvaria (data not shown).

Peroxisomal protein import and mitochondrial structure are not affected in *PEX11*β$^{-/-}$ mice. Zellweger syndrome and its corresponding mouse models display a number of cellular abnormalities. Chief among these is the inability to import peroxisomal matrix enzymes (11). However, enzyme import appears to be unaffected in *PEX11*β$^{-/-}$ cells. This is shown here by the cytochemical detection of the peroxisomal marker enzyme catalase (imported through the PTS1 pathway) within hepatocyte peroxisomes of *PEX11*β$^{-/-}$ mice (Fig. 4A and B), as well as the colocalization of the peroxisomal enzyme catalase and the peroxisomal membrane protein PEX14 in *PEX11*β$^{-/-}$ MEF (Fig. 4C to F). An enzyme imported through the PTS2 pathway, phytanoyl coenzyme A hydroxylase, was also targeted into peroxisomes when expressed as a myc-tagged form in *PEX11*β$^{-/-}$ MEF (Fig. 4G and H), demonstrating that all peroxisomal protein import pathways are functional in cells lacking PEX11β. Nevertheless, the loss of *PEX11*β did appear to reduce peroxisome abundance and increase peroxisome clustering (Fig. 5A) and elongation (Fig. 4F and 5B). Defects in mitochondrial structure have also been reported in Zellweger syndrome patients and Zellweger syndrome mice (3, 10), but these too were absent from *PEX11*β$^{-/-}$ hepatocytes (Fig. 5C), although we did detect mitochondrial proliferation in some cells (Fig. 4B and 5C). Zellweger syndrome is also characterized by hepatic accumulation of VLCFAs (36, 38), a substrate of the peroxisomal β-oxidation pathway, which is thought to explain the presence of needle-like lipid crystals on the surface of hepatocyte lipid droplets and within phagosomes of Kupffer cells (the resident macrophages of the liver) in mouse models of Zellweger syndrome (3). We found no evidence of such needle-like lipid crystals in the livers of *PEX11*β$^{-/-}$ mice (Fig. 5D to F).

VLCFA accumulation is not responsible for neuronal abnormalities in *PEX11*β$^{-/-}$ mice. The diagnosis of Zellweger syndrome is typically confirmed by biochemical tests (24, 38). In Zellweger syndrome patients and prior mouse models of Zellweger syndrome, VLCFA levels are 10 times higher than normal and plasmalogen levels are 10 to 100 times lower than normal (3, 9, 24). By contrast, *PEX11*β$^{-/-}$ mice have normal levels of brain VLCFAs, no alteration of hepatic plasmalogens, and only slight alterations of hepatic VLCFAs (1.4×) and brain plasmalogens (0.8×) (Fig. 6A and C). We also measured rates of VLCFA β-oxidation and plasmalogen synthesis in cultured fibroblasts. Relative to controls, we detected no change in plasmalogen synthesis rates and only a slight decrease in VLCFA β-oxidation, to 0.6× that of normal controls (Fig. 6B and D). Some Zellweger syndrome patients accumulate the branched-chain fatty acids phytanic acid and pristanic acid, which are substrates of the peroxisomal fatty acid α- and β-oxidation pathways, respectively, and the oxidation of these substrates is typically impaired in Zellweger syndrome fibroblasts (11, 25, 37). *PEX11*β$^{-/-}$ animals, on the other hand, do not accumulate these fatty acids in the liver (Fig. 6E) or other tissues (data not shown), and *PEX11*β$^{-/-}$ fibroblasts have normal oxidation activities toward both phytanic and pristanic acids (Fig. 6F).

DISCUSSION

Peroxisomal enzyme import defects are the root cause of all known instances of Zellweger syndrome and prior mouse models of Zellweger syndrome (11). *PEX11*β deficiency has most of the pathological hallmarks of Zellweger syndrome, including a neuronal migration defect, enhanced neuronal apoptosis, a

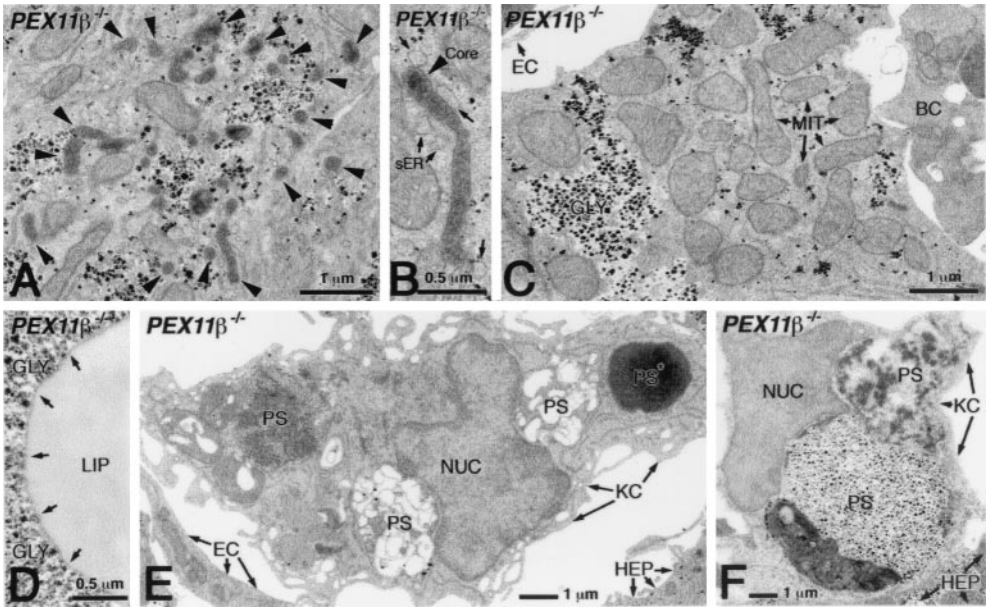

FIG. 5. No mitochondrial defects or lipid crystals in *PEX11*β$^{-/-}$ mouse liver. Ultrastructural analysis of DAB-stained preparations (postfixation and with aqueous osmium) revealed elevated peroxisome clustering (A) and elongation (B) in some hepatocytes of *PEX11*β$^{-/-}$ mice. Arrowheads indicate the positions of peroxisomes, and arrows in panel B show the position of smooth endoplasmic reticulum (sER). (C) Hepatocytes of *PEX11*β$^{-/-}$ mice had no mitochondrial structural abnormalities, although in some cells they did appear to be more abundant than in those of controls. MIT, mitochondria; GLY, glycogen; EC, endothelial cell; BC, blood cell. (D) Hepatocytes of *PEX11*β$^{-/-}$ mice lacked needle-like crystals on the surface of their lipid droplets (D; arrows show where large, needle-like crystals would be seen in Zellweger syndrome patients and mice). (E and F) VLCFA crystals were also absent from phagosomes (PS) of Kupffer cells (KC). NUC, nucleus of a Kupffer cell; EC, endothelial cell; HEP, hepatocyte; PS*, red blood cell in a phagosome. Note the high level of phagocytic degradation of different blood cells in phagosomes (E) and the occasional phagocytosis of hepatocytes (F) in Kupffer cells of *PEX11*β$^{-/-}$ mice.

developmental delay, neonatal hypotonia, and neonatal lethality, without the peroxisomal enzyme import defects that are the cellular hallmarks of this disease. *PEX11*β deficiency also differs from Zellweger syndrome with regard to peroxisomal metabolic defects. Zellweger syndrome patients and prior mouse models of Zellweger syndrome show 1,000% increases in VLCFAs, a marker substrate of the peroxisomal β-oxidation pathway, and 90 to 99% decreases in plasmalogens, a marker product of the peroxisomal ether lipid synthesis pathway (3, 9, 24). In contrast, *PEX11*β$^{-/-}$ mice have no alteration in brain VLCFAs or liver plasmalogens, only a slight increase (~40%) in liver VLCFAs, a slight decrease (~20%) in brain plasmalogens, and no accumulation of peroxisomal fatty acid α-oxidation substrates. In cultured cells, *PEX11*β deficiency has no effect on plasmalogen synthesis and no effect on phytanic acid and pristanic acid oxidation and causes only a slight decrease (~40%) in VLCFA β-oxidation. Thus, *PEX11*β deficiency represents a novel peroxisomal disorder that mimics major neurological and developmental pathologic features of Zellweger syndrome but lacks many of its cellular and biochemical features.

It is important to note that *PEX11*β-deficient mice lack several other features of Zellweger syndrome, such as facial dysmorphism, enlarged cranial fontanelles, and renal cysts (23). However, these pathologic features were also absent from prior mouse models of Zellweger syndrome (3, 9). One reasonable explanation for these differences is that both Zellweger syndrome mice and *PEX11*β-deficient mice die very shortly after birth, precluding the development of what may be later-stage pathologic features. The severe kidney and bone development delay we observed in *PEX11*β-deficient mice may be an early manifestation of these deficiencies.

Although there is no firm hypothesis about exactly which substrate, product, or combination of substrates and products is the etiologic agent of Zellweger syndrome, patients who are defective in the peroxisomal β-oxidation enzyme D-bifunctional protein (D-BP) (14, 38) have clinical phenotypes in common with Zellweger syndrome patients. In contrast, patients with defects in ether lipid synthesis or fatty acid α-oxidation are associated with distinct phenotypes (38, 39). These and other observations have led to the hypothesis that Zellweger syndrome pathologic features might be induced primarily by their severe fatty acid β-oxidation defect and perhaps by VLCFA toxicity (28). With regard to VLCFA toxicity, *PEX11*β$^{-/-}$ mice have only a very mild accumulation of VLCFAs (~40%), which is far less severe than the VLCFA accumulation of Zellweger syndrome mice (~1,000%). VLCFA accumulation in *PEX11*β$^{-/-}$ mice is also less severe than the 200 to 300% increase in VLCFAs observed in *ALD*-deficient mice, which have no detectable pathologic features (20, 26). Thus, it appears that the developmental delay, neuronal migration defects, enhanced neuronal apoptosis, neonatal hypotonia, and neonatal lethality of *PEX11*β deficiency cannot be explained by VLCFA toxicity. With regard to the hypothesis that Zellweger syndrome pathologic features are caused primarily by defects in peroxisomal β-oxidation, the phenotypes of *PEX11*β$^{-/-}$ mice are distinct from those of mice lacking the peroxisomal β-oxidation enzyme D-BP (4). In par-

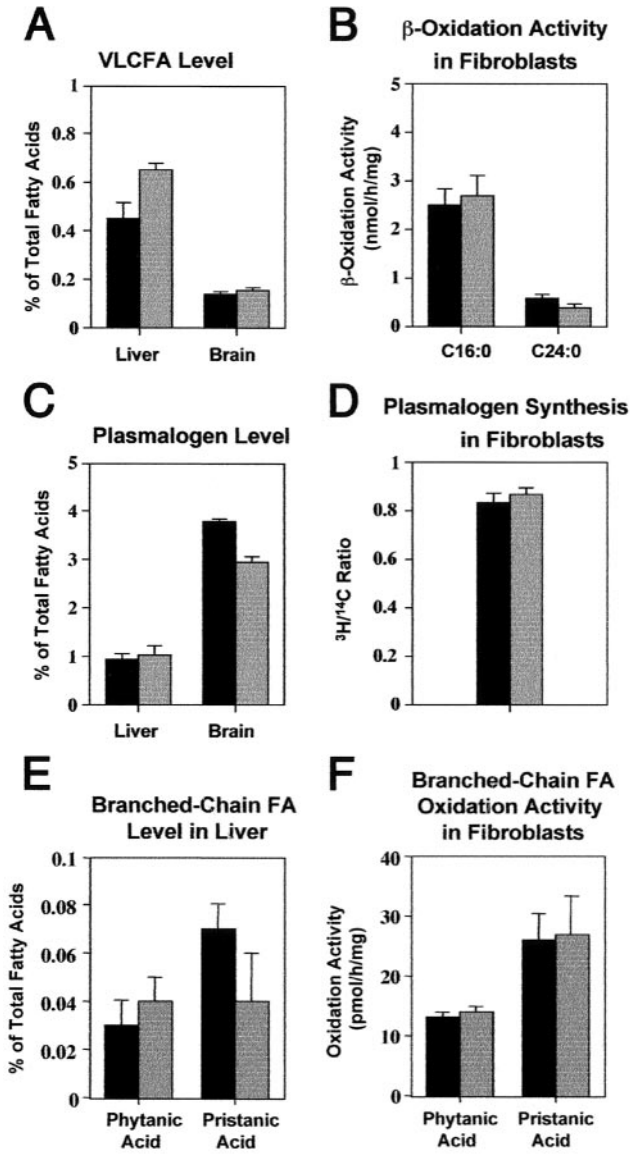

FIG. 6. *PEX11*β$^{-/-}$ mice have a mild, generalized defect in peroxisome metabolism. In all of the graphs, black bars represent average values obtained with *PEX11*β$^{+/+}$, gray bars represents average values obtained with *PEX11*β$^{-/-}$, and brackets represent 1 standard deviation. Abundance of VLCFAs (A) and activities of mitochondrial ($C_{16:0}$) and peroxisomal ($C_{24:0}$) fatty acid β-oxidation (B) in cultured MEF. (C) Plasmalogens in control and *PEX11*β$^{-/-}$ mice, expressed as percentages of the total fatty acids. (D) Plasmalogen synthesis activities in cultured MEF, expressed as the ratio of peroxisomal incorporation of [^{14}C]hexadecanol to endoplasmic reticulum incorporation of [^{3}H]hexadecyl-glycerol. (E) Levels of the branched-chain fatty acids phytanic acid and pristanic acid in the liver. (F) Rates of phytanic acid and pristanic acid oxidation in cultured fibroblasts from mutant and control animals.

ticular, *PEX11*β-deficient mice do not display the nearly total defect in VLCFA oxidation and branched-chain (pristanic) fatty acid oxidation of D-BP-deficient mice.

The exceedingly mild metabolic defects in *PEX11*β$^{-/-}$ mice raise the interesting possibility that the pathologic features of these mice, and perhaps Zellweger syndrome mice and Zellweger syndrome patients, are not caused by nonspecific metabolite toxicity. Rather, it may be that the metabolic abnormalities of these diseases impair animal development through a subtle, yet inappropriate, activation or inactivation of one or more signaling pathways in the body. Peroxisomal metabolic pathways play critical roles in the synthesis of many signaling lipids, including ligands of nuclear hormone receptors RXR, PPARα, and PPARγ (15–17). If true, this pathogenic hypothesis raises the possibility of therapeutic interventions that could normalize the putative signaling pathways and the development of these animals. Future studies of animals should allow us to test this hypothesis directly, as well as its relevance to Zellweger syndrome pathogenesis.

Our results also have implications for the disparate topics of Zellweger syndrome diagnosis and PEX11 function. Current diagnostic procedures for Zellweger syndrome and other peroxisomal disorders (24, 38) would incorrectly exclude a generalized peroxisomal dysfunction in a patient with *PEX11*β deficiency, even though these patients display defects in two unrelated peroxisomal metabolic pathways. Therefore, we propose that current diagnostic protocols be modified to include the possibility of *PEX11*β deficiency in the human population. With regard to the molecular role of PEX11β and other PEX11 proteins in peroxisome biogenesis, there are two competing hypotheses. One predicts that PEX11 proteins play an important role in peroxisome division (6, 12, 21), and the other holds that PEX11 proteins play a direct role in medium-chain fatty acid oxidation and affect peroxisome abundance only indirectly (35). This issue was addressed in detail in a previous report, which concluded that PEX11 proteins act directly in peroxisome division (18). This conclusion is supported by the observation here that *PEX11*β$^{-/-}$ mice are defective in two unrelated peroxisomal metabolic pathways, a strong indicator that PEX11β plays a more direct role in peroxisome biogenesis than peroxisomal metabolism.

Although the loss of *PEX11*β is lethal, *PEX11*β$^{-/-}$ mice still contain an intact *PEX11*α gene and do not lack PEX11 activity altogether. In fact, the loss of *PEX11*β induces a slight increase (~1.5×) in hepatic expression of *PEX11*α (data not shown). A more complete understanding of PEX11 function in mammals requires the generation and analysis of mice lacking all *PEX11* genes.

ACKNOWLEDGMENTS

We thank the Johns Hopkins University Transgenic Core Facility for blastocyst injections and generation of chimeric animals, Ann and Hugo Moser for the use of their laboratory for biochemical experiments, and Stephanie Mihalik and Paul Watkins for help with the peroxisomal α- and β-oxidation activity measurements.

This work was supported by grants from the National Institutes of Health to S.J.G. (DK59479) and D.V. (HD10981). D.V. is an investigator of the Howard Hughes Medical Institute. E.B. was supported by a Max-Kade Scholarship (Max-Kade Foundation, New York, N.Y., and Deutsche Forschungsgemeinschaft).

REFERENCES

1. **Abe, I., and Y. Fujiki.** 1998. cDNA cloning and characterization of a constitutively expressed isoform of the human peroxin Pex11p. Biochem. Biophys. Res. Commun. **252:**529–533.
2. **Abe, I., K. Okumoto, S. Tamura, and Y. Fujiki.** 1998. Clofibrate-inducible, 28-kDa peroxisomal integral membrane protein is encoded by PEX11. FEBS Lett. **431:**468–472.
3. **Baes, M., P. Gressens, E. Baumgart, P. Carmeliet, M. Casteels, M. Fransen, P. Evrard, D. Fahimi, P. E. Declercq, D. Collen, P. P. van Veldhoven, and G. P. Mannaerts.** 1997. A mouse model for Zellweger syndrome. Nat. Genet. **17:**49–57.

4. **Baes, M., S. Huyghe, P. Carmeliet, P. E. Declercq, D. Collen, G. P. Mannaerts, and P. P. Van Veldhoven.** 2000. Inactivation of the peroxisomal multifunctional protein-2 in mice impedes the degradation of not only 2-methyl-branched fatty acids and bile acid intermediates but also of very long chain fatty acids. J. Biol. Chem. **275:**16329–16336.
5. **Baumgart, E., I. Vanhorebeek, M. Grabenbauer, M. Borgers, P. E. Declercq, H. D. Fahimi, and M. Baes.** 2001. Mitochondrial alterations caused by defective peroxisomal biogenesis in a mouse model for Zellweger syndrome (PEX5 knockout mouse). Am. J. Pathol. **159:**1477–1494.
6. **Erdmann, R., and G. Blobel.** 1995. Giant peroxisomes in oleic acid-induced *Saccharomyces cerevisiae* lacking the peroxisomal membrane protein Pmp27p. J. Cell Biol. **128:**509–523.
7. **Evan, G. E., G. K. Lewis, G. Ramsay, and J. M. Bishop.** 1985. Isolation of monoclonal antibodies specific for human c-myc proto-oncogene product. Mol. Cell. Biol. **5:**3610–3616.
8. **Fahimi, H. D.** 1969. Cytochemical localization of peroxidatic activity of catalase in rat hepatic microbodies (peroxisomes). J. Cell Biol. **43:**275–288.
9. **Faust, P. L., and M. E. Hatten.** 1997. Targeted deletion of the PEX2 peroxisome assembly gene in mice provides a model for Zellweger syndrome, a human neuronal migration disorder. J. Cell Biol. **139:**1293–1305.
10. **Goldfischer, S., C. L. Moore, A. B. Johnson, A. J. Spiro, M. P. Valsmis, H. K. Wisniewski, R. H. Ritch, W. T. Norton, I. Rapin, and L. M. Gartner.** 1973. Peroxisomal and mitochondrial defects in the cerebro-hepato-renal syndrome. Science **182:**62–64.
11. **Gould, S. G., D. Valle, and G. V. Raymond.** 2001. The peroxisome biogenesis disorders, p. 3181–3217. *In* C. R. Scriver, A. L. Beaudet, W. S. Sly, and D. Valle (ed.), The metabolic and molecular bases of inherited disease, 8th ed., vol. 2. McGraw-Hill, New York, N.Y.
12. **Gould, S. J., and D. Valle.** 2000. The genetics and cell biology of the peroxisome biogenesis disorders. Trends Genet. **16**:340–344.
13. **Hogan, B., R. Beddington, F. Costantini, and E. Lacy.** 1994. Manipulating the mouse embryo: a laboratory manual, 2nd ed. Cold Spring Harbor Laboratory Press, Cold Spring Harbor, N.Y.
14. **Kaufmann, W. E., C. Theda, S. Naidu, P. A. Watkins, A. B. Moser, and H. W. Moser.** 1996. Neuronal migration abnormality in peroxisomal bifunctional enzyme defect. Ann. Neurol. **39:**268–271.
15. **Kersten, S., B. Desvergne, and W. Wahli.** 2000. Roles of PPARs in health and disease. Nature **405:**421–424.
16. **Kitareewan, S., L. T. Burka, K. B. Tomer, C. E. Parker, L. J. Deterding, R. D. Stevens, B. M. Forman, D. E. Mais, R. A. Heyman, T. McMorris, and C. Weinberger.** 1996. Phytol metabolites are circulating dietary factors that activate the nuclear receptor RXR. Mol. Biol. Cell **7:**1153–1166.
17. **Lemotte, P. K., S. Keidel, and C. M. Apfel.** 1996. Phytanic acid is a retinoid X receptor ligand. Eur. J. Biochem. **236:**328–333.
18. **Li, X., and S. G. Gould.** 2002. PEX11 promotes peroxisome division independently of peroxisome metabolism. J. Cell Biol. **156:**643–651.
19. **Lorenz, P., A. G. Maier, E. Baumgart, R. Erdmann, and C. Clayton.** 1998. Elongation and clustering of glycosomes in Trypanosoma brucei overexpressing the glycosomal Pex11p. EMBO J. **17:**3542–3555.
20. **Lu, J. F., A. M. Lawler, P. A. Watkins, J. M. Powers, A. B. Moser, H. W. Moser, and K. D. Smith.** 1997. A mouse model for X-linked adrenoleukodystrophy. Proc. Natl. Acad. Sci. USA **94:**9366–9371.
21. **Marshall, P., Y. Krimkevich, R. Lark, J. Dyer, M. Veenhuis, and J. Goodman.** 1995. Pmp27 promotes peroxisomal proliferation. J. Cell Biol. **129:**345–355.
22. **Mihalik, S., J. Morrell, D. Kim, K. Sacksteder, P. Watkins, and S. Gould.** 1997. Identification of PAHX as a Refsum disease gene. Nat. Genet. **17:**185–189.
23. **Moser, A., M. Rasmussen, S. Naidu, P. Watkins, M. McGuinness, A. Hajra, G. Chen, G. Raymond, A. Liu, D. Gordon, K. Garnaas, D. Walton, O. Okjeldal, M. Guggenheim, L. Jackson, E. Elias, and H. Moser.** 1995. Phenotype of patients with peroxisomal disorders subdivided into sixteen complementation groups. J. Pediatr. **127:**13–22.
24. **Moser, A. B., N. Kreiter, L. Bezman, S. Lu, G. V. Raymond, S. Naidu, and H. W. Moser.** 1999. Plasma very long chain fatty acids in 3,000 peroxisome disease patients and 29,000 controls. Ann. Neurol. **45:**100–110.
25. **Moser, H. W.** 1999. Genotype-phenotype correlations in disorders of peroxisome biogenesis. Mol. Genet. Metab. **68:**316–327.
26. **Moser, H. W., K. D. Smith, P. A. Watkins, J. Powers, and A. B. Moser.** 2001. X-linked adrenoleukodystrophy, p. 3257–3301. *In* C. R. Scriver, A. L. Beaudet, W. S. Sly, and D. Valle (ed.), The metabolic and molecular bases of inherited disease, 8th ed., vol. 2. McGraw-Hill, New York, N.Y.
27. **Passreiter, M., M. Anton, D. Lay, R. Frank, C. Harter, F. T. Wieland, K. Gorgas, and W. W. Just.** 1998. Peroxisome biogenesis: involvement of ARF and coatomer. J. Cell Biol. **141:**373–383.
28. **Powers, J. M., and H. W. Moser.** 1998. Peroxisomal disorders: genotype, phenotype, major neuropathologic lesions, and pathogenesis. Brain Pathol. **8:**101–120.
29. **Roscher, A., B. Molzer, H. Bernheimer, S. Stockler, I. Mutz, and F. Paltauf.** 1985. The cerebrohepatorenal (Zellweger) syndrome: an improved method for the biochemical diagnosis and its potential value for prenatal detection. Pediatr Res. **19:**930–933.
30. **Sacksteder, K. A., and S. J. Gould.** 2000. The genetics of peroxisome biogenesis. Annu. Rev. Genet. **34:**623–652.
31. **Sacksteder, K. A., J. M. Jones, S. T. South, X. Li, Y. Liu, and S. J. Gould.** 2000. PEX19 binds multiple peroxisomal membrane proteins, is predominantly cytoplasmic, and is required for peroxisome membrane synthesis. J. Cell Biol. **148:**931–944.
32. **Sakai, Y., P. A. Marshall, A. Saiganji, K. Takabe, H. Saiki, N. Kato, and J. M. Goodman.** 1995. The *Candida boidinii* peroxisomal membrane protein Pmp30 has a role in peroxisomal proliferation and is functionally homologous to Pmp27 from *Saccharomyces cerevisiae*. J. Bacteriol. **177:**6773–6781.
33. **Sambrook, J., E. Fritsch, and T. Maniatis.** 1989. Molecular cloning: a laboratory manual, 2nd ed. Cold Spring Harbor Laboratory Press, Cold Spring Harbor, N.Y.
34. **Schrader, M., B. E. Reuber, J. C. Morrell, G. Jimenez-Sanchez, C. Obie, T. Stroh, D. Valle, T. A. Schroer, and S. J. Gould.** 1998. Expression of *PEX11*β mediates peroxisome proliferation in the absence of extracellular stimuli. J. Biol. Chem. **273:**29607–29614.
35. **van Roermund, C. W., H. F. Tabak, M. van Den Berg, R. J. Wanders, and E. H. Hettema.** 2000. Pex11p plays a primary role in medium-chain fatty acid oxidation, a process that affects peroxisome number and size in Saccharomyces cerevisiae. J. Cell Biol. **150:**489–498.
36. **Wanders, R. J., and J. M. Tager.** 1998. Lipid metabolism in peroxisomes in relation to human disease. Mol. Aspects Med. **19:**69–154.
37. **Wanders, R. J., P. Vreken, S. Ferdinandusse, G. A. Jansen, H. R. Waterham, C. W. van Roermund, and E. G. Van Grunsven.** 2001. Peroxisomal fatty acid alpha- and beta-oxidation in humans: enzymology, peroxisomal metabolite transporters and peroxisomal diseases. Biochem. Soc. Trans. **29:**250–267.
38. **Wanders, R. J. A., P. G. Barth, and H. S. A. Heymans.** 2001. Single peroxisomal enzyme deficiencies, p. 3219–3256. *In* C. R. Scriver, A. L. Beaudet, W. S. Sly, and D. Valle (ed.), The metabolic and molecular bases of inherited disease, 8th ed., vol. 2. McGraw-Hill, New York, N.Y.
39. **Wanders, R. J. A., C. Jakobs, and O. H. Skejldal.** 2001. Refsum disease, p. 3303–3322. *In* C. R. Scriver, A. L. Beaudet, W. S. Sly, and D. Valle (ed.), The metabolic and molecular bases of inherited disease, 8th ed., vol. 2. McGraw-Hill, New York, N.Y.
40. **Wang, T., A. M. Lawler, G. Steel, and D. Valle.** 1995. Paradoxical hypoornithenemia and neonatal lethality in mice with targeted disruption of the OAT gene. Nat. Genet. **11:**185–190.
41. **Watkins, P., E. J. Ferrell, J. Pedersen, and G. Hoefler.** 1991. Peroxisomal fatty acid β-oxidation in HepG2 cells. Arch. Biochem. Biophys. **289:**329–366.
42. **Zenger-Hain, J., D. A. Craft, and W. B. Rizzo.** 1992. Diagnosis of inborn errors of phytanic acid oxidation with tritiated phytanic acid. Prog. Clin. Biol. Res. **375:**399–407.